The ectoine hydroxylase: a nonheme-containing iron(II) and 2-oxoglutarate-dependent dioxygenase

Nils Widderich[†,‡], *Erhard Bremer*[†,‡], *and Sander HJ Smits*[*]

[†]Department of Biology, Laboratory for Microbiology, Philipps-University Marburg, Marburg, Germany
[‡]LOEWE-Center for Synthetic Microbiology, Philipps-University Marburg, Marburg, Germany
[*]Institute for Biochemistry, Heinrich-Heine-University Düsseldorf, Düsseldorf, Germany

FUNCTIONAL CLASS

Enzyme; nonheme-containing iron(II) and 2-oxoglutarate-dependent dioxygenase superfamily (EC 1.14.11). Members of this superfamily are versatile catalysts whose enzyme reactions include hydroxylations, dimethlyations, desaturations, epimerizations, cyclizations, halogenations, and ring expansions. Described here is the ectoine hydroxylase (EctD) that converts ectoine to 5-hydroxyectoine in an iron(II)-dependent manner.

The enzyme EctD hydroxylates ectoine *via* a region-selective and stereospecific enzymatic reaction forming the stress-protectant and chemical chaperone 5-hydroxyectoine [(4*S*,5*S*)-2-methyl-5-hydroxy-1,4,5,6-tetrahydropyrimidine-4-carboxylic acid].[1,2]

OCCURRENCE

Synthesis of ectoine [(*S*)-2-methyl-1,4,5,6-tetrahydropyrimidine-4-carboxylic acid] ensues from L-aspartate-β-semialdehyde, a central intermediate in microbial amino acid metabolism and cell wall synthesis, and comprises the sequential activities of the L-2,4-diaminobutyrate transaminase (EctB; EC 2.6.1.76), 2,4-diaminobutyrate acetyltransferase (EctA; EC 2.3.1.178), and ectoine synthase (EctC; EC 4.2.1.108). The ectoine derivative

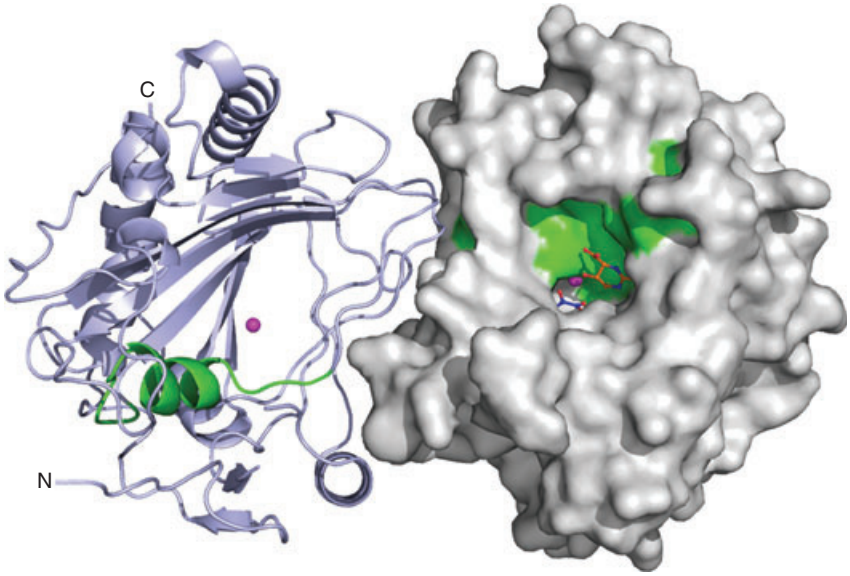

3D Structure Structure of the dimeric ectoine hydroxylase from *S. alaskensis* (*Sa*EctD). One monomer is represented as cartoon representation. The other monomer is highlighted as a surface with the bound 2-oxoglutarate substrate (shown as blue sticks) and the 5-hydroxyectoine product (shown in orange). The bound Fe(II) ligand is shown as spheres colored in magenta (PDB code: 4Q5O). The signature sequence motif of *Sa*EctD is colored in green. These figures were prepared using PyMOL (www.pymol.org).

This article was published in the *Encyclopedia of Inorganic and Bioinorganic Chemistry* in 2016 by John Wiley & Sons, Ltd.
DOI: 10.1002/9781119951438.eibc2440

5-hydroxyectoine [(4*S*,5*S*)-5-hydroxy-2-methyl-1,4,5,6-tetrahydropyrimidine-4-carboxylic acid] is formed only by a subgroup of the ectoine producers and is catalyzed by the ectoine hydroxylase (EctD) (EC 1.14.11). The expression of the ectoine biosynthetic genes (*ectABC*) is typically osmotically induced and this operon might also comprise the structural gene (*ectD*) for the ectoine hydroxylase. However, *ectD* genes are also often found separated from the *ectABCD* gene cluster.[1,3,4] In a recent survey of putative hydroxyectoine-producing microorganisms, 72% possess *ectD* genes that are located next to the *ectABC* gene cluster. The highest number of *ectD* genes are observed in the actinobacterial ectoine producers, in particular, in strains of the genera *Streptomyces*, *Actinomadura*, fast-growing species of *Mycobacterium*, in most species of the orders *Pseudonocardiales*, *Glycomycetales*, the genus *Nocardiopsis*, and the phylogenetically basal genus *Nitriliruptor*. There are only eight archaeal representatives predicted to synthesize 5-hydroxyectoine. Each of these is a member of the aerobic thaumarchaeal genus *Nitrosopumilus*[5] and they share very similar *ectD* gene products with those of the gamma proteobacterial genus *Nitrosococcus*. As the ectoine hydroxylase is oxygen dependent,[1,6] it is not surprising that no *ectD* gene is found in any of the anaerobic ectoine-producing bacterial or archaeal microorganisms. The EctD protein is frequently misannotated in genome sequences as proline hydroxylases or phytanoyl hydroxylases that, similar to the ectoine hydroxylase, also belong to the nonheme-containing iron(II) and 2-oxoglutarate-dependent dioxygenase superfamily.[7–9] *Bona fide* EctD-type proteins can, however, easily be distinguished from other members of the nonheme-containing iron(II) and 2-oxoglutarate-dependent dioxygenase superfamily by the presence of a highly conserved signature sequence motif.[1,10] This 17-amino acid region is highly conserved in the all analyzed ectoine hydroxylases, contains amino acids functionally important for iron and substrate bindings, and is an important determinant for the overall structure of the ectoine hydroxylase (see below).[6,11]

BIOLOGICAL FUNCTION

Ectoine (Figure 1) is a well-recognized compatible solute and microbial stress protectant.[12,13] It is synthesized widely by members of the *Bacteria* and a few *Archaea*[5,11,13,14] as an adaptive response to osmotic stress[1,14–20] and growth-restricting extremes in high and low temperatures.[4,17] Some ectoine producers[11] also synthesize a derivative of ectoine, in which a hydroxy group is stereospecifically attached to the pro-*S* hydrogen at position C5 in the tetrahydropyrimidine ring to yield 5-hydroxyectoine (Figure 1). This reaction is carried out by the ectoine hydroxylase EctD. 5-hydroxyectoine is often superior to its precursor molecule ectoine in protecting microorganisms against environmentally imposed stresses.[4,18]

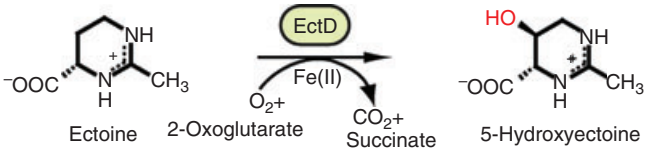

Figure 1 Scheme of the EctD-catalyzed reaction. The iron(II) containing ectoine hydroxylase converts ectoine, molecular oxygen, and 2-oxoglutarate into 5-hydroxyectoine, CO_2, and succinate.

AMINO ACID SEQUENCE INFORMATION

The following nine EctD proteins have been biochemically characterized (accession codes are derived from the UniProt database). Eight are derived from members of the *Bacteria* and one is derived from the Thaumarchaeon *N. maritimus*:

- *Halomonas elongata: He*EctD; 332 amino acids; p*I*: 5.8, protein accession code: CBV43892.
- *Acidiphilium cryptum: Ac*EctD; 306 amino acids; p*I*: 5.8, protein accession code: ABQ32201.
- *Alkalilimnicola ehrlichii: Ae*EctD; 302 amino acids; p*I*: 5.7, protein accession code: AER00257.
- *Sphingopyxis alaskensis: Sa*EctD; 306 amino acids; p*I*: 5.5, protein accession code: ABF54657.
- *Paenibacillus lautus: Pl*EctD; 302 amino acids; p*I*: 5.6, protein accession code: ACX67869.
- *Pseudomonas stutzeri: Ps*EctD; 302 amino acids; p*I*: 5.5, protein accession code: CBM40642.
- *Virgibacillus salexigens: Vs*EctD; 300 amino acids; p*I*: 5.8, protein accession code: AY935522.
- *Streptomyces coelicolor: Sc*EctD; 299 amino acids; p*I*: 5.1, protein accession code: Q93RV9.
- *Nitrosopumilus maritimus*: *Nm*EctD; 304 amino acids; p*I*: 5.8, protein accession code: ABX13239.

These nine EctD proteins display a degree of amino acid sequence identity between 66% and 35% toward each other. Amino acids involved in binding the Fe(II) cofactor, the cosubstrate 2-oxoglutarate, and the substrate ectoine are highly conserved in the large EctD protein family.[11]

PROTEIN PRODUCTION AND PURIFICATION

So far, nine ectoine hydroxylases have been characterized biochemically.[1,5,11] To overexpress these proteins, the corresponding *ectD* genes were either amplified from genomic DNA of the corresponding microorganisms or synthesized as codon-optimized versions for their expression in *Escherichia coli*. They were cloned into the pASK-IBA3 overexpression vector (IBA GmbH, Göttingen, Germany) and placed under the transcriptional control

This article was published in the *Encyclopedia of Inorganic and Bioinorganic Chemistry* in 2016 by John Wiley & Sons, Ltd.
DOI: 10.1002/9781119951438.eibc2440

of the TetR-responsive and anhydrotetracycline (AHT)-inducible *tet*-promoter. The resulting EctD proteins contain a *Strep*-tag affinity peptide at their carboxy terminal end to allow purification by affinity chromatography. EctD proteins have been successfully overproduced in *E. coli* BL21 cells. For these experiments, cultures were grown at 37 °C and 180 rpm until they reached an OD_{578} of 0.5; subsequently, the temperature and the shaking speed were reduced to 30 °C and 100 rpm, respectively. At OD_{578} of 0.7, overexpression of the *ectD* genes was induced by the addition of AHT. After 2 h of further growth, cells were harvested and pellets were frozen and stored at −80 °C until further usage.

For purification of the EctD proteins, the pellets were resuspended in 20 mM 2-[[1,3-dihydroxy-2-(hydroxymethyl)propan-2-yl]amino]ethanesulfonic acid (TES), pH 8, 100 mM KCl and were then disrupted by passing them three times through a French Pressure Cell Press. Cellular debris was removed by ultracentrifugation and the cleared supernatant was loaded onto a Strep-Tactin Superflow column that had been equilibrated with five bed volumes of the resuspension buffer (20 mM TES, pH 8, 100 mM KCl). The column was then washed with 10 column volumes of resuspension buffer. The EctD proteins were eluted from the affinity chromatography material with three column volumes of resuspension buffer that contained 2.5 mM desthiobiotin. The eluted EctD proteins were concentrated with Vivaspin 6 columns to a final concentration of about 5–10 mg ml^{-1}. Two hundred to three hundred milligrams EctD protein was routinely obtained through this overproduction and purification scheme per liter of cell culture for the codon-optimized genes, whereas nonoptimized version obtained about 50–100 mg. The protein concentration was measured using the Pierce™ BCA Protein Assay Kit (Thermo Scientific, Schwerte, Germany) and the specific extinction coefficient at 280 nm and the specific molecular mass of the full length EctD proteins including the *Strep*-tagII affinity peptide (Table 1).

ACTIVITY ASSAY

The enzymatic activity of the EctD proteins and their mutants was assayed in 30 µl reaction volumes that typically contained 10 mM TES buffer (pH 7.5), 10 mM 2-oxoglutarate, 6 mM ectoine, 1 mM $FeSO_4$, and various amounts of the purified EctD protein. Once the optimal conditions with respect to temperature, pH value, and salt concentration had been determined, the kinetic parameters the EctD enzyme for its cosubstrate 2-oxoglutarate, and its substrate ectoine were determined. The enzyme reaction mixtures were incubated at 32 °C for 20 min in a thermomixer (Eppendorf, Hamburg, Germany) with vigorous shaking providing enough oxygen for the O_2-dependent EctD enzyme. The enzyme reactions were stopped by the addition of 30 µl of 100% acetonitrile to the reaction mixtures and the samples were then immediately centrifuged (10 min, 4 °C, 32 000*g*) to remove the denatured EctD protein. Formation of 5-hydroxyectoine from the substrate ectoine was determined by loading 20 µl of the supernatant of the cleared enzyme reaction mixture onto a GROM-SIL 100 Amino-1PR column (125 mm by 4 mm; 3-µm particle size) (GROM, Rottenburg-Hailfingen, Germany) attached to a UV–visible detector system (LINEAR UVIS 205; SYKAM, Fürstenfeldbruck, Germany) and using 80% acetonitrile as the running solvent. Ectoine and 5-hydroxyectoine can readily be separated from each other by this chromatographic procedure (Figure 2). By observing their absorbance at 210 nm,[1,16] the amounts of the remaining ectoine and that of the newly formed 5-hydroxyectoine can be quantitated with the ChromStar 7.0 software package (SYKAM, Fürstenfeldbruck, Germany). Known quantities of commercial available ectoine and hydroxyectoine reference compounds (http://www.bitop.de/cms/website.php?id=/de/index/extremolyte.htm) were used as benchmarks to assess the catalytic efficiency of the various studied EctD enzymes.

MOLECULAR CHARACTERIZATION

Most of the studied ectoine hydroxylases have been characterized biochemically and kinetically (Table 1) in a similar

Table 1 Kinetic parameters of investigated ectoine hydroxylases[5,11,18]

EctD from	Length (AA)	MW (kDa)	p*I*	K_m (mM ectoine)	V_{max} (U/mg)	k_{cat} (s^{-1})	K_m (mM 2-oxoglutarate)
V. salexigens	300	34.4	5.8	5.9 ± 0.3	6.4 ± 0.2	3.2	4.9 ± 0.3
S. alaskensis	306	34.1	5.5	9.8 ± 0.5	1.0 ± 0.2	1.7	2.7 ± 0.3
H. elongata	332	37.4	5.8	5.7 ± 0.6	2.5 ± 0.2	1.0	4.8 ± 0.4
P. stutzeri	302	34.2	5.5	6.2 ± 0.4	6.7 ± 0.2	3.6	4.6 ± 0.5
P. lautus	302	34.8	5.6	9.5 ± 0.7	1.3 ± 0.1	0.6	3.9 ± 0.2
A. ehrlichii	302	34.3	5.7	9.0 ± 0.3	1.0 ± 0.1	0.7	5.0 ± 0.3
A. cryptum	306	34.1	5.8	10.0 ± 0.6	2.8 ± 0.3	2.3	4.1 ± 0.4
N. maritimus	304	34.7	5.8	3.8 ± 0.5	1.8 ± 0.1	1.0	3.1 ± 0.6
S. coelicolor	299	32.9	5.1	2.6 ± 0.2	20 ± 1	–	6.2 ± 0.2

This article was published in the *Encyclopedia of Inorganic and Bioinorganic Chemistry* in 2016 by John Wiley & Sons, Ltd.
DOI: 10.1002/9781119951438.eibc2440

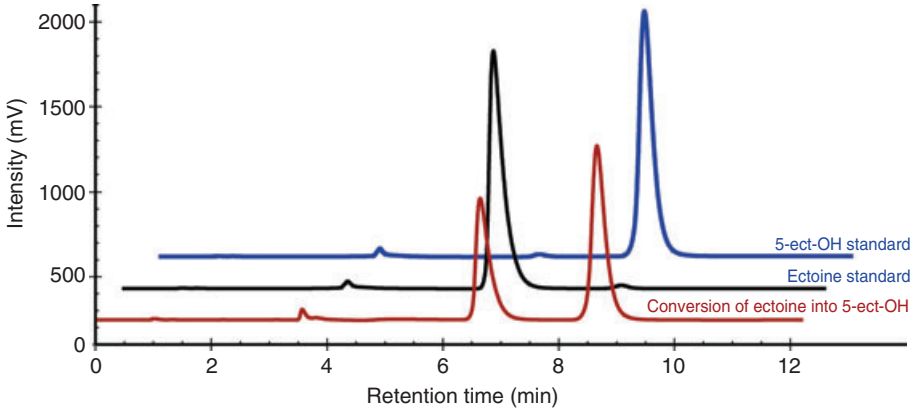

Figure 2 Representative HPLC chromatograms of ectoine and 5-hydroxyectoine. Standard solutions of ectoine (black) and 5-hydroxyectoine (blue) are depicted and a representative chromatogram of an *in vitro* conversion of ectoine into 5-hydroxyectoine (red) by the purified *Sa*EctD enzyme is shown.

way, allowing a direct comparison of enzymes originating from microorganisms living in rather different habitats and members from both the bacterial and archaeal kingdoms.[1,5,11] The temperature and pH optima ranged between 30 and 40 °C and 7.0 and 8.0, respectively, and each of the enzymes could be activated by the addition of salts. With respect to their kinetic parameters, their affinity (K_m) values for ectoine ranged between 5.5 and 10.0 mM and their maximal activity (V_{max}) between 1.0 and 7.0 U/mg of protein (Table 1). Despite the fact that the original host organisms for the studied EctD proteins belong to different bacterial phyla and inhabit diverse ecological niches, the biochemical and kinetic properties of the different studied ectoine hydroxylases are very similar.[1,5,11] Hence, the properties of the so far studied nine ectoine hydroxylases can probably be regarded as representative for the entire extended EctD protein family.[5,11]

METAL CONTENT

Biochemical and structural assessment of the ectoine hydroxylases revealed that the enzyme belongs to the nonheme-containing iron(II) and 2-oxoglutarate-dependent dioxygenase superfamily.[1,10,21] Hence, the EctD enzyme possesses iron(II) as its cofactor. Presence of iron in EctD protein preparations was determined using a photometric assay described by Lovenberg *et al.*[22] In this assay, 10 nmol of the proteins were heated at 80 °C in 1% HCl for denaturation of the protein. The iron content of the samples was then determined by the addition of phenanthroline, which, in complex with iron, adopts a purple/red color that can be measured photometrically at 512 nm. Performing such an assay with the different, in *E. coli* recombinantly produced EctD proteins, resulted in an iron content of roughly 85–95%.

X-RAY STRUCTURES

Crystallization of *Vs*EctD and *Sa*EctD

The EctD enzyme has been crystallized from two different microorganisms, the cold-adapted *Sphingopyxis alaskensis* (*Sa*EctD) and the salt-tolerant *Virgibacillus salexigens* (*Vs*EctD). The *Sa*EctD protein was quite challenging to crystallize, and most of the crystals obtained in the initial screen were of low quality. To obtain better quality crystals, the detergent screens from Hampton Research, Aliso Viejo, USA, were used as described.[23] After several rounds of optimization and buffer adjustments, crystals for X-ray crystallography were obtained, which finally resulted in structures of *Sa*EctD in the apo- and iron-bound form. The crystallization procedures are described in detail below.

Apo-*Sa*EctD: crystallization trials were performed using the sitting-drop vapor diffusion method at 20 °C. 1.5 µl of the homogenous protein solution of *Sa*EctD (10 mg ml^{-1} in 20 mM TES, pH 7.5, 80 mM NaCl) was mixed with 1.5 µl reservoir solution containing 100 mM 2-(N-morpholino)ethanesulfonic acid (MES), pH 6.0, 200 mM Ca-acetate, 27–32% (w/v) polyethyleneglycol (PEG) 400, and 1.5 mM *n*-dodecyl-*N*,*N*-dimethylglycine and equilibrated over 300 µl reservoir solution. Crystals grew within 6–12 days to their final size of around 30 µm × 30 µm × 50 µm. This resulted in crystals exhibiting a C222 symmetry with a unit cell of $a = 83.48$ Å, $b = 86.51$ Å, $c = 95.34$ Å, and $\alpha = \beta = \gamma = 90°$. These crystals diffracted to a resolution of 2.1 Å and one monomer of the apo-*Sa*EctD appeared to be present in the asymmetric unit (ASU) of the crystal.

Crystallization of the *Sa*EctD protein in complex with its iron catalyst was carried out as described above for apo-*Sa*EctD protein except that the protein solution was premixed with $Fe(II)Cl_2$ (final concentration of 4 mM) and equilibrated for 10–15 min on ice. In addition, the solution contained 3.5 mM n-dodecyl-N,N-dimethylglycine.

This article was published in the *Encyclopedia of Inorganic and Bioinorganic Chemistry* in 2016 by John Wiley & Sons, Ltd.
DOI: 10.1002/9781119951438.eibc2440

Crystals grew within 6–12 days at 20 °C to their final size of around 40 μm × 40 μm × 180 μm. These types of crystals diffracted to 2.6 Å resolution and exhibited an orthorhombic $P2_12_12_1$ symmetry with a unit cell of $a = 78.16$ Å, $b = 87.52$ Å, $c = 96.05$ Å, and $\alpha = \beta = \gamma = 90°$. Two monomers of *Sa*EctD were present in the ASU of the crystal. The crystal contact was mediated by n-dodecyl-N,N-dimethylglycine, a compound that had been added to the *Sa*EctD protein before crystallization.

To obtain a view of the ligand binding within the *Sa*EctD protein, crystallization was performed with the cosubstrate 2-oxoglutarate and the reaction product 5-hydroxyectoine. Using this combination, it was believed that the *Sa*EctD protein would be arrested in a ligand bound state, which then can be used for crystallization. Unfortunately, the conditions found for the apo- and Fe-bound *Sa*EctD structure did not yield crystals diffracting to high resolution. Furthermore, the structure calculated from the collected datasets (at a maximum of 4.2–4.5 Å) revealed that none of the two ligands was present within the crystal.

To achieve this, another intensive round of screening was necessary to obtain crystals of *Sa*EctD in complex with Fe, 2-oxoglutarate, and 5-hydroxyectoine. Finally, this succeeded by adding the substrates sequentially, as done before to obtain crystals of other protein–ligand complexes.[24] The *Sa*EctD protein was mixed with $Fe(II)Cl_2$ as described and subsequently 2-oxoglutarate was added to the *Sa*EctD to a final concentration of 40 mM. After 30 min of incubation on ice, the third compound, 5-hydroxyectoine was added to the solution at a final concentration of 40 mM. This mixture was then incubated for 1 h on ice before crystallization trials were conducted. The order in which the ligands were added to the protein solution appeared to be crucial. Substrate-bound *Sa*EctD crystals were grown by mixing 1.5 μl protein solution with 1.5 μl reservoir containing 100 mM MES, pH 6.0, 200 mM Ca-acetate, 30% (w/v) PEG 400, and 25 mM *n*-Octyl-β-D-glycoside. After 6–12 days, they reached their final size of around 40 μm × 40 μm × 70 μm. All crystals were cryoprotected by carefully adding 1 μl of 100% glycerol to the crystallization drop before the crystals were frozen in liquid nitrogen. This crystal diffracted to 2.6 Å resolution and exhibited an orthorhombic $P2_12_12_1$ symmetry with a unit cell of $a = 81.00$ Å, $b = 87.08$ Å, $c = 94.88$ Å, and $\alpha = \beta = \gamma = 90°$. A functional dimer was present in the ASU.

Overall structure of ectoine hydroxylases

The core of nonheme-containing iron(II) and 2-oxoglutarate-dependent dioxygenase[8,9,25] is comprised of mainly antiparallel β-strands that fold to form a distorted/squashed barrel-like structure open at one end allowing the substrate to diffuse into the active center. This barrel-like structure is also termed 'cupin fold'.[8,9] The amino acid sequences of the *Vs*EctD and *Sa*EctD proteins described here possess an amino acid sequence identity of 51%. An overall comparison of the five determined EctD crystal structures from *Vs*EctD and *Sa*EctD (PDB accession codes: 3EMR, 4NMI, 4MHR 4MHU, and 4Q5O) revealed a high degree of identity with a root–mean–square deviation (r.m.s.d.) that ranges from 1.3 to 1.6 Å over 279 Cα atoms. An even lower RMSD of 0.5–0.9 Å was found when the three different *Sa*EctD structures or the two *Vs*EctD structures were compared with each other.

As the monomers of all known EctD structures are nearly identical in overall shape, we describe in the following section only the overall fold for the apo-*Sa*EctD protein. The *Sa*EctD crystal structure consists of a double-stranded β-helix core surrounded and stabilized by a number of α-helices (3D Structure). This core, termed the jelly-roll or cupin fold,[8,9] is formed by two four-stranded antiparallel β-sheets that are arranged in the form of a β-sandwich. This type of architecture has previously been observed not only for the EctD proteins[10,11,21,23] but also for many other nonheme-containing iron(II) and 2-oxoglutarate-dependent dioxygenases.[8,9,26] This is highlighted by a DALI search,[27] which revealed structural similarity of EctD to the human phytanoyl-CoA hydroxylases PhyH (PDB code 2A1X; r.m.s.d of 2.6 Å over 252 C-alpha atoms when compared to the *Sa*EctD structure)[28] PhyHD1A (PDB code 2OPW r.m.s.d. of 2.2 Å over 286 Cα atoms),[29] the halogenases SyrB2 from *Pseudomonas syringae* (PDB code 2FCV; r.m.s.d. of 2.9 Å over 299 Cα atoms),[30] CytC3 from a *Streptomyces* soil isolate (PDB code 3GJA; r.m.s.d. of 3.0 Å over 204 C-alpha atoms),[31] and CurA from the cyanobacterium *Lyngbya majuscula* (PDB code 3NNM; r.m.s.d. of 3.3 Å over 222 Cα atoms).[32] While the core of the cupin-type fold of EctD is highly similar to these proteins, the rest of the EctD protein differs from the structurally compared proteins resulting in higher r.m.s.d. values.

Alignments of the amino acid sequences of over 400 ectoine hydroxylases revealed a highly conserved signature sequence motif of 17 amino acids in length (FXWHSDFETWHXEDGM/LP).[1,6,10,11,18] This string of amino acids forms an extended α-helix followed by a short β-strand; it structures one side of the EctD cupin-barrel (highlighted in green in 3D Structure). The signature sequence region is structurally important for the overall fold of the EctD proteins and notably contains five residues that contribute to the binding of all three ligands of the ectoine hydroxylase: Fe(II), 2-oxoglutarate, and ectoine. In the *Sa*EctD protein, these residues comprise the side chains of His144 and Asp146 involved in iron binding, Phe141 involved in 2-oxoglutarate binding, and His144, Asp146, Thr149, and Trp150 that are involved in binding and the correct positioning of the substrate ectoine.

*Sa*EctD contains a large loop (amino acids 191–210), which is disordered and hence not visible in the electron density map. By amino acid sequence alignment, this loop corresponds to residues 195–211 in the *Vs*EctD ectoine hydroxylase and it is disordered in both available crystal structures.[10,11] Interestingly, in the ligand-free crystal

This article was published in the *Encyclopedia of Inorganic and Bioinorganic Chemistry* in 2016 by John Wiley & Sons, Ltd.
DOI: 10.1002/9781119951438.eibc2440

structures of the phytanoyl-CoA hydroxylase PhyH,[28] the asparagine hydroxylase AsnO from *Streptomyces coelicolor*,[33] the L-arginine oxygenase VioC from *Streptomyces vinaceus*,[34] and the taurine dioxygenases from *E. coli* and *Pseudomonas putida*,[35] a similar loop is disordered as well and became only visible in crystal structures with bound substrates. It is thought that this mobile loop functions as a lid that shields the active site form the solvent once the ligands are bound.

Oligomeric state: EctD is a dimeric protein

To determine the oligomeric state of the purified *Sa*EctD in solution, we carried out high-pressure liquid chromatography coupled to multiangle light scattering (HPLC-MALS) analysis. This method allows the calculation of the size of the particle (or protein) running through the column. The normalized elution profiles from the UV, refractive index, and light scattering detectors revealed that the protein solution was homogeneous and monodisperse. After determining protein concentration by the refractive index, a molecular mass of 70.73 ± 1.1 kDa was obtained for the *Sa*EctD protein.[21] This molecular mass corresponds very well with the theoretical molecular mass of a dimer of the recombinant protein (calculated molecular mass of the monomer, including the Strep-tag-II affinity peptide: 35.29 kDa).[21] Hence, *Sa*EctD is a dimer in solution, in line with the result obtained for six other EctD proteins as assessed by conventional size-exclusion chromatography.[11] HPLC-MALS analysis of the *Sa*EctD protein was repeated in the presence of the 2-oxoglutarate and ectoine substrates revealing that *Sa*EctD was a dimer under these conditions as well. Overall, these data suggest that the hydroxylation of ectoine is mediated by a dimeric EctD enzyme.

The crystal structures of *Sa*EctD and *Vs*EctD displayed a different crystal packing (as observed by the different symmetries of the crystals) and protein composition in the ASU of the crystals. Inspection of the crystal packing and analysis of the monomer–monomer interactions in the crystals revealed a physiological relevant dimer (Figure 1).[21] Using the PDBe PISA software,[36] 10 potential amino acids were identified to be involved in monomer–monomer interaction. Each of these is located in loop areas pointing from one monomer toward the other and thereby contributes to the formation of the dimer interface. These amino acids are, however, only moderately conserved, as judged by consulting an alignment of over 400 EctD-type proteins.[6,11]

Iron-binding site in *Sa*EctD and *Vs*EctD

Both *Vs*EctD and *Sa*EctD were crystallized in the Fe(II) bound state. In *Vs*EctD, the iron cofactor is coordinated by the side chains of His146, Asp148, and His248, together with three water molecules that interact with the iron ligand, arranged in an almost perfect octahedral geometry (Figure 3(a)).[10] To probe the functional role of His146, Asp148, and His248 in *Vs*EctD for iron-binding and enzyme activity,[1] Ala mutants were created for each of the three iron-binding residues. These *Vs*EctD variants neither were able to bind iron nor were they enzymatically active. These residues form a structurally strictly conserved HXD/E…H motif, the 2-His-1-carboxylate facial triad, forming a type of mononuclear iron center that can be found in many members of the dioxygenase superfamily.[7–9,26] The structure of *Sa*EctD revealed a set of interactions involved in binding the Fe(II) ion similar to that found in the *Vs*EctD protein (Figure 3(a)). However, in the *Sa*EctD structure, no water molecules were observed near the iron ligand owing to the moderate 2.6 Å resolution of this structure.[21] In other EctD-related protein structures adopting a cupin fold, which were identified by a structural comparison search using the DALI server (Table 2), the Fe(II) ligand is bound *via* a octahedral geometry as well.

Crystal structures of EctD were also obtained in the unliganded apo form. Comparison of the structural arrangement in the apo- and iron-bound structure of *Vs*EctD and *Sa*EctD revealed no significant structural differences. This highlights that the iron ligand does not induce significant structural changes in the ectoine hydroxylase up on binding, rather the iron-binding site is preset of receive the Fe(II) cofactor.[21]

Mechanistic aspects

Unfortunately, no crystal structure of the substrate-bound form of *Vs*EctD has been reported. To get a glimpse of the Fe(II)-binding site in the presence of 2-oxoglutarate, structural alignments were preformed with members of the nonheme-containing iron(II) and 2-oxoglutarate-dependent dioxygenases crystallized in complex with either 2-oxoglutarate or analogs of this cosubstrate.[37,38] This suggested a binding site in *Vs*EctD for this cosubstrate similar to that experimentally determined in other nonheme-containing iron(II) and 2-oxoglutarate-dependent dioxygenases. In this *in silico* model, the 2-oxoglutarate interacts twice with the Fe(II) atom and replaces the water molecules observed in the Fe(II) crystal structure by which the octahedral conformation of the metal remains (Figure 3(b)) and Table 2).

While no 2-oxoglutarate-bound *Vs*EctD crystal structure could be obtained, that of *Sa*EctD was solved with 2-oxoglutarate, and in the presence of the product 5-hydroxyectoine, the so-called dead-end enzyme state. In this structure, the binding site of 2-oxoglutarate was confirmed to be similar to the binding site observed in other 2-oxoglutarate-dependent dioxygenases, including that predicted *in silico* for the *Vs*EctD protein. In addition to the interactions with the side chains of His144, His245,

This article was published in the *Encyclopedia of Inorganic and Bioinorganic Chemistry* in 2016 by John Wiley & Sons, Ltd.
DOI: 10.1002/9781119951438.eibc2440

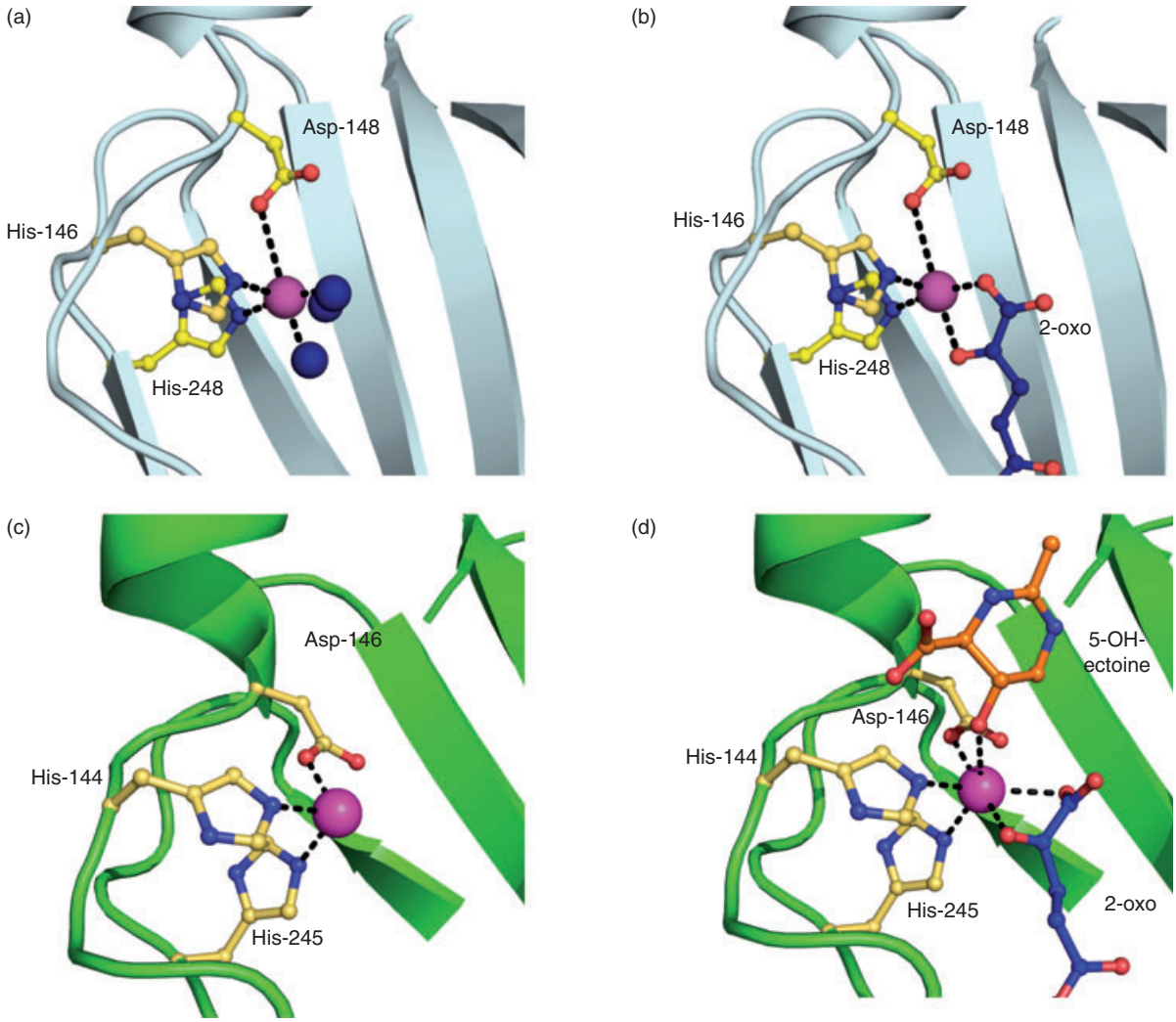

Figure 3 Iron-binding site in *Vs*EctD and *Sa*EctD. (a) The iron-binding site of *Vs*EctD is highlighted. The octahedral coordination of Fe(II) is mediated by His146, Asp148, His248, H_2O-823, H_2O-824, and H_2O-824. All distances of the side chain atoms toward the Fe(II) ligand are in between 2.3 and 2.6 Å. (b) Architecture of the Fe(II)-binding site in the apo-*Sa*EctD structure. The coordination of Fe(II) is mediated by His144, Asp146, and His245. The resolution of this structure does not allow the placing of water molecules and therefore no further interaction partners are observed. All distances of the side chain atoms toward the Fe(II) ligand are in between 2.3 and 2.7 Å. (c) The Fe(II)-binding site in the *Sa*EctD in complex with 2-oxoglutarate and 5-hydroxyectoine is depicted. (d) The octahedral coordination of Fe(II) is mediated by His144, Asp146, His245, 2-oxoglutarate, and 5-hydroxyectoine. All distances of the side chain atoms toward the Fe(II) ligand are in between 2.3 and 2.6 Å. The PDB accession codes used in this figure are 3EMR, 4NMI, 4MHU, and 4Q5O.

and Asp146 and with 2-oxoglutarate, one further interaction appeared to be present in this dead-end complex. Fe(II) interacted with the 5-hydroxy group present in the product 5-hydroxyectoine as expected for an enzyme reaction mechanisms directly involved the Fe(II) ion (Figure 3(b)).

On the basis of the crystal structures, the biochemical studies with the EctD protein, and in analogy with other nonheme-containing iron(II) and 2-oxoglutarate-dependent dioxygenases,[6,7,9,25,39,40] the following enzyme reaction (Figure 4) for the ectoine hydroxylase was proposed: (**I**) The substrate-free EctD enzyme contains Fe(II), sixfold-coordinated by the 2-His-1-carboxylate facial triad formed by His146, Asp148, and His248, and three water molecules.[10] Two of the water molecules are replaced from the iron center upon addition of 2-oxoglutarate. Subsequently, the substrate ectoine is envisioned to bind to the EctD enzyme *via* the molecular interactions gleaned from the *Sa*EctD:5-hydroxyectoine complex. (**II**) Upon substrate binding, dioxygen replaces the third water molecule from the iron center and oxidizes Fe(II) to Fe(IV). (**III**) The formed Fe(IV)-peroxo species attacks with its anion the carbonyl-C atom of 2-oxoglutarate to yield succinate, CO_2, and the ferryl species (Fe(IV)═O).[41] The ferryl species hydroxylates ectoine to (*4S*,*5S*)-5-hydroxyectoine. (**IV**) This

This article was published in the *Encyclopedia of Inorganic and Bioinorganic Chemistry* in 2016 by John Wiley & Sons, Ltd.
DOI: 10.1002/9781119951438.eibc2440

Table 2 Structures of known EctD enzymes and proteins adopting a similar fold as deduces from a DALI search

Enzyme	PDB code	Ligand	Metal-binding site	Binding geometry
*Vs*EctD	3emr	Fe(II)	His146, Asp148, His248, H_2O-823, H_2O-824, H_2O-824	Octahedral
*Sa*EctD	4mhu	Fe(II)	His144, Asp146, His245	Square planar[a]
*Sa*EctD	4q5o	Fe(II), 2-oxo, 5-hydroxyectoine	His144, Asp146, His245, 2oxo, 5hydroxyectoine	Octahedral
PhyH	2a1x	Fe(II), 2-oxo	His175, Asp177, His264, 2oxo, H_2O-463	Octahedral
Avi01	4xaa	Ni(II)	His125, Asp127, His196, H_2O-426, H_2O-429, H_2O-440	Octahedral
Evd01	4xbz	Ni(II)	His139, Asp141, His223, glycerol-402	Octahedral
SyrB2	2fct	Fe(II), 2-oxo	His116, His235, 2-oxo, chloride ion	Octahedral
FtmOx1	4y5s	Fe(II), 2-oxo	His133, Asp135, His209, 2-oxo	Octahedral
HygX	4xca	Ni(II), 2-oxo	His102, His205, 2-oxo, H_2O-458, H_2O-459	Octahedral
CytC3	3gjb	Fe(II), 2-oxo	His118, His240, 2-oxo, H_2O-402, H_2O-400	Octahedral
CurA	3nnf	Fe(III), 2-oxo	His115, His228, cloride-321, 2-oxo, FMT	Octahedral
PtlH	2rdq	Fe(III), 2-oxo	His137, Asp139, His226, 2-oxo, H_2O-270	Octahedral
Phd2	3ouj	Fe(III), 2-oxo	His313, Asp315, His374, 2-oxo, H_2O-23	Octahedral

The binding geometry was calculated using the CMM software.[37]
[a]For the *Sa*EctD structure, a geometry was calculated to be square planar.

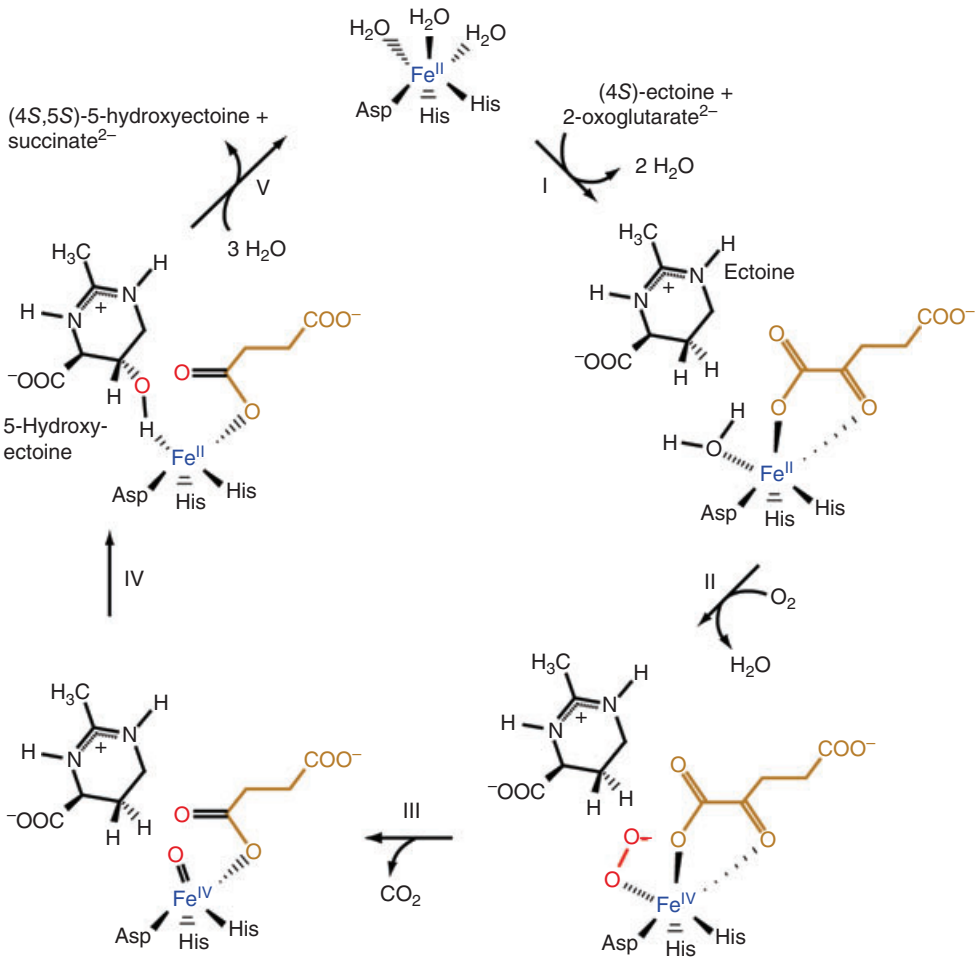

Figure 4 Proposal for the reaction mechanism of the conversion of ectoine into 5-hydroxyectoine by the ectoine hydroxylase.[6] For a detailed explanation see text.

This article was published in the *Encyclopedia of Inorganic and Bioinorganic Chemistry* in 2016 by John Wiley & Sons, Ltd.
DOI: 10.1002/9781119951438.eibc2440

may occur either by abstraction of the pro-*S* hydrogen at C5 by Fe(IV)═O and readdition of the hydroxyl radical from Fe(III)—OH to the ectoine radical intermediate with retention of the configuration (rebound mechanism) or by insertion of the ferryl oxygen atom into the C—H bond (two-state reactivity mechanism). (V) Finally, the product (*4S*,*5S*)-5-hydroxyectoine and the coproduct succinate are released. Three water molecules will then occupy again the empty coordination site of Fe(II).

Role of the ectoine hydroxylase

Ectoine and 5-hydroxyectoine are potent osmostress protectants for microorganisms and also serve as protectants against extremes in growth temperature. They can exert these functions both when they are synthesized and when they are imported *via* osmotically controlled transport systems.[13] Increased production of 5-hydroxyectoine often occurs when the growth of osmotically stressed microbial cells slows down and the culture enters stationary phase, indicating that the cytoprotective effects of 5-hydroxyectoine go beyond its well-known function as an osmostress protectant. Indeed, the EctD-catalyzed hydroxylation of ectoine endows the newly formed 5-hydroxyectoine with properties that are often superior to that exhibited by ectoine; for example, 5-hydroxyectoine provides enhanced heat-stress protection[4,18,38] and it is also a very effective protectant against desiccation in comparison with ectoine. This latter property is caused by the ability of 5-hydroxyectoine to form glass-like structures.[38] The question therefore arises, why do not all ectoine-producing bacteria[5,11] also produce 5-hydroxyectoine? Part of the answer can readily be deduced from the biochemical properties of the ectoine hydroxylase as it is a strictly oxygen-dependent enzyme.[1,5,11] Microorganisms with an anaerobic metabolism could therefore not make use of it, as highlighted by the recent study of ectoine-producing members of the *Archaea*.[5] As members of the *Methanosaeta* and *Methanobacterium* genera are all strict anaerobes, the absence of *ectD* in the genomes of these methanogens is readily understandable. On the other hand, the presence of *ectD* genes in *Nitrosopumilus maritimus* SCM1, other members of the *Nitrosopumilus* genus, and related Marine Group I Thaumarchaeota is consistent with the lifestyle of these *Archaea* as oxygen-dependent nitrifying microorganisms.[5]

The crystallographic analysis of the Fe-(*Sa*)EctD/2-oxoglutarate/5-hydroxyectoine complex provided a detailed snapshot of the architecture of the active site of the ectoine hydroxylase. Synthetic ectoine derivatives with either reduced or expanded ring sizes have been reported.[42,43] The architecture of the catalytic core of the EctD protein[21] is probably flexible enough to allow the hydroxylation of synthetic, ectoine-related molecules. An EctD-mediated hydroxylation might endow them with novel stress-protective and structure-preserving functions in the same way that it allows 5-hydroxyectoine to function strikingly different from ectoine in alleviating desiccation stress.[38] As a result, the EctD enzyme is not only of interest from an ecophysiological and biotechnological point of view,[5,11–13] it also has the potential for use in chemical biology.

RELATED ARTICLES

2,3-Dihydroxybiphenyl 1,2-Dioxygenase; Naphthalene 1,2-Dioxygenase; Iron Proteins with Dinuclear Active Sites

REFERENCES

1 J Bursy, AJ Pierik, N Pica and E Bremer, *J Biol Chem*, **282**, 31147–31155 (2007).
2 L Inbar, F Frolow and A Lapidot, *Eur J Biochem*, **214**, 897–906 (1993).
3 J Prabhu, F Schauwecker, N Grammel, U Keller and M Bernhard, *Appl Environ Microbiol*, **70**, 3130–3132 (2004).
4 R Garcia-Estepa, M Argandona, M Reina-Bueno, N Capote, F Iglesias-Guerra, JJ Nieto and C Vargas, *J Bacteriol*, **188**, 3774–3784 (2006).
5 N Widderich, Czech L, F J Elling, M Koenneke, N Stoeveken, M Pittelkow, R Riclea, J S Dickschat, J Heider, E Bremer, *Environ Microbiol(*2015), doi: 10.1111/1462-2920.13156. [Epub ahead of print] PMID: 26636559.
6 N Widderich, M Pittelkow, A Höppner, D Mulnaes, W Buckel, H Gohlke, SH Smits and E Bremer, *J Mol Biol*, **426**(3), 586–600 (2014).
7 RP Hausinger, *Crit Rev Biochem Mol Biol*, **39**, 21–68 (2004).
8 W Aik, MA McDonough, A Thalhammer, R Chowdhury and CJ Schofield, *Curr Opin Struct Biol*, **22**, 691–700 (2012).
9 JA Hangasky, CY Taabazuing, MA Valliere and MJ Knapp, *Metallomics*, **5**, 287–301 (2013).
10 K Reuter, M Pittelkow, J Bursy, A Heine, T Craan and E Bremer, *PLoS One*, **5**, e10647 (2010).
11 N Widderich, A Höppner, M Pittelkow, J Heider, SHJ Smits and E Bremer, *PLoS One*, **9**, e93809 (2014).
12 G Lentzen and T Schwarz, *Appl Microbiol Biotech*, **72**, 623–634 (2006).
13 JM Pastor, M Salvador, M Argandona, V Bernal, M Reina-Bueno, LN Csonka, JL Iborra, C Vargas, JJ Nieto and M Canovas, *Biotechnol Adv*, **28**, 782–801 (2010).
14 K Schwibbert, A Marin-Sanguino, I Bagyan, G Heidrich, G Lentzen, H Seitz, M Rampp, SC Schuster, HP Klenk, F Pfeiffer, D Oesterhelt and HJ Kunte, *Environ Microbiol*, **13**, 1973–1994 (2011).
15 P Louis and EA Galinski, *Microbiology*, **143**, 1141–1149 (1997).
16 AU Kuhlmann and E Bremer, *Appl Environ Microbiol*, **68**, 772–783 (2002).
17 AU Kuhlmann, J Bursy, S Gimpel, T Hoffmann and E Bremer, *Appl Environ Microbiol*, **74**, 4560–4563 (2008).

This article was published in the *Encyclopedia of Inorganic and Bioinorganic Chemistry* in 2016 by John Wiley & Sons, Ltd.
DOI: 10.1002/9781119951438.eibc2440

18 J Bursy, AU Kuhlmann, M Pittelkow, H Hartmann, M Jebbar, AJ Pierik and E Bremer, *Appl Environ Microbiol*, **74**, 7286–7296 (2008).

19 SH Saum and V Muller, *Environ Microbiol*, **10**, 716–726 (2008).

20 II Mustakhimov, AS Reshetnikov, AS Glukhov, VN Khmelenina, MG Kalyuzhnaya and YA Trotsenko, *J Bacteriol*, **192**, 410–417 (2010).

21 A Hoppner, N Widderich, M Lenders, E Bremer and SH Smits, *J Biol Chem*, **289**, 29570–29583 (2014).

22 W Lovenberg, BB Buchanan and JC Rabinowitz, *J Biol Chem*, **238**, 3899–3913 (1963).

23 A Hoeppner, N Widderich, E Bremer and SH Smits, *Acta Crystallogr F Struct Biol Commun*, **70**, 493–496 (2014).

24 A Hoeppner, L Schmitt, S H Smits, Proteins and Their Ligands: Their Importance and How to Crystallize Them. Intech Books, Vol. **II**, pp. 44 (2013), Available from: http://www.intechopen.com/books/advanced-topics-on-crystal-growth/proteins-and-their-ligands-their-importance-and-how-to-crystallize-them.

25 AG Prescott and MD Lloyd, *Nat Prod Rep*, **17**, 367–383 (2000).

26 S Kundu, *BMC Res Notes*, **5**, 410 (2012).

27 L Holm and P Rosenström, *Nucl Acids Res*, **38**, W545–W549 (2010).

28 MA McDonough, KL Kavanagh, D Butler, T Searls, U Oppermann and CJ Schofield, *J Biol Chem*, **280**, 41101–41110 (2005).

29 Z Zhang, GT Kochan, SS Ng, KL Kavanagh, U Oppermann, CJ Schofield and MA McDonough, *Biochem Biophys Res Commun*, **408**, 553–558 (2011).

30 LC Blasiak, FH Vaillancourt, CT Walsh and CL Drennan, *Nature*, **440**, 368–371 (2006).

31 C Wong, DG Fujimori, CT Walsh and CL Drennan, *J Am Chem Soc*, **131**, 4872–4879 (2009).

32 D Khare, B Wang, L Gu, J Razelun, DH Sherman, WH Gerwick, K Hakansson and JL Smith, *Proc Natl Acad Sci U S A*, **107**, 14099–14104 (2010).

33 M Strieker, F Kopp, C Mahlert, LO Essen and MA Marahiel, *ACS Chem Biol*, **2**, 187–196 (2007).

34 V Helmetag, SA Samel, MG Thomas, MA Marahiel and LO Essen, *FEBS J*, **276**, 3669–3682 (2009).

35 SH Knauer, O Hartl-Spiegelhauer, S Schwarzinger, P Hanzelmann and H Dobbek, *FEBS J*, **279**, 816–831 (2012).

36 E Krissinel and K Henrick, *J Mol Biol*, **372**, 774–797 (2007).

37 H Zheng, MD Chordia, DR Cooper, M Chruszcz, P Muller, GM Sheldrick and W Minor, *Nat Protoc*, **9**, 156–170 (2014).

38 C Tanne, EA Golovina, FA Hoekstra, A Meffert and EA Galinski, *Front Microbiol*, **5**, 150 (2014).

39 GD Straganz and B Nidetzky, *Chembiochem*, **7**, 1536–1548 (2006).

40 PK Grzyska, EH Appelman, RP Hausinger and DA Proshlyakov, *Proc Natl Acad Sci U S A*, **107**, 3982–3987 (2010).

41 PJ Riggs-Gelasco, JC Price, RB Guyer, JH Brehm, EW Barr, JM Bollinger Jr, and C Krebs, *J Am Chem Soc*, **126**, 8108–8109 (2004).

42 M Schnoor, P Voss, P Cullen, T Boking, HJ Galla, EA Galinski and S Lorkowski, *Biochem Biophys Res Commun*, **322**, 867–872 (2004).

43 EM Witt, NW Davies and EA Galinski, *Appl Microbiol Biotechnol*, **91**, 113–122 (2011).

This article was published in the *Encyclopedia of Inorganic and Bioinorganic Chemistry* in 2016 by John Wiley & Sons, Ltd.
DOI: 10.1002/9781119951438.eibc2440